Fish and Shellfish Immunology 94 (2019) 17–26

Contents lists available at ScienceDirect

Fish and Shellfish Immunology

journal homepage: www.elsevier.com/locate/fsi

Full length article

Dynamic immune and metabolism response of clam *Meretrix petechialis* to *Vibrio* challenge revealed by a time series of transcriptome analysis

Jiajia Yu[a,c], Hongxia Wang[a,b], Xin Yue[a,b], Baozhong Liu[a,b,c,*]

[a] CAS Key Laboratory of Experimental Marine Biology, Institute of Oceanology, Center for Ocean Mega-Science, Chinese Academy of Sciences, Qingdao, 266071, China
[b] Laboratory for Marine Biology and Biotechnology, Qingdao National Laboratory for Marine Science and Technology, Qingdao, 266000, China
[c] University of Chinese Academy of Sciences, Beijing, 100049, China

ARTICLE INFO

Keywords:
Meretrix petechialis
Vibrio
DEGs
Innate immunity
Anabolism

ABSTRACT

Meretrix petechialis is an important commercial aquaculture species in China. During the clam culture period, mass mortality events often occurred due to the *Vibrio* infection. In this paper, *M. petechialis* were challenged with *Vibrio parahaemolyticus* immersion to simulate a natural infection, and the infection process were divided into four phases including latency, prodrome, onset and recovery phases based on the clam mortality data. Then, the dynamic response of clams to *Vibrio* infection at different infection phases were investigated by transcriptome analysis. A total of 38,067 differentially expressed genes (DEGs) were identified at different infection phases. DEG annotations showed that immune-related and metabolism-related signaling pathways were enriched, indicating that immune defense and metabolism process play key roles during bacterial infection. Three kinds of expression pattern were classified by cluster analysis, including U-shape, L-shape and inverted V-shape. Anabolism and cellular growth proliferation related signaling pathways were repressed (long-lasting or transient) during bacterial infection. However, the immune related signaling pathways with different immune functions showed induction expression or repression expression against bacterial infection, which indicated that immune system take different strategies against bacterial infection. Furthermore, some signaling pathways such as PI3K-Akt signaling pathway both involved in immune defense and cell metabolism. This study provides a sight that the dynamic immunity and metabolic responses may be integrated to improve the host survival and shift more energy for immune defense.

1. Introduction

The clam *Meretrix petechialis*, an important commercial aquaculture species, is major cultured in the coastal areas of South and Southeast Asia [1]. In recent years, with the improvement of artificial seed-rearing techniques, the aquaculture production of *M. petechialis* has greatly increased [2,3]. However, mass mortality events often occurred during the process of clam culture due to the excessive breeding density and various pathogenic bacteria. Previous studies have shown that *Vibrio* is a main pathogen causing mass mortality of cultured clams [4,5]. But little is known about the molecular mechanisms underlying the immune defense response to pathogenic bacterial infection in this bivalve species, which hindering the formulation of effective measures for disease prevention and control in clam culture [6].

As an invertebrate, *M. petechialis* mainly depends on innate immune to defense bacteria or virus infection. Innate immune system is composed of cellular and humoral component to combat pathogen, remove pathogen and repair tissue [7–9]. In our laboratory, several immune-related genes in *M. petechialis*, including lysozyme, catalase (CAT) and glutathione peroxidase (GPx), etc., were identified and characterized with regard to their involvement in immune response to bacterial infection [10–12]. Moreover, Jiang et al. [6] identified 14 immune-related genes response to bacterial infection by transcriptome analysis. However, these studies about *M. petechialis* immune system most focus on single gene or single time point, which not allow us to identify the spatial regulation network and the temporal events. It is necessary to investigate the dynamic variation of gene expression across the whole infection phases, which could provide a global understanding for the immune defense of clams against bacterial infection [13].

RNA-seq is commonly used to investigate the transcription of genes and major pathways involved in disease process, metabolism process

* Corresponding author. CAS Key Laboratory of Experimental Marine Biology, Institute of Oceanology, Center for Ocean Mega-Science, Chinese Academy of Sciences, Qingdao, 266071, China.
E-mail address: bzliu@qdio.ac.cn (B. Liu).

https://doi.org/10.1016/j.fsi.2019.08.057
Received 14 June 2019; Received in revised form 20 August 2019; Accepted 24 August 2019
Available online 26 August 2019

and reproduction, etc. at the overall level [14–17]. In recent years, RNA-seq has been widely used in mollusks immune related research. Transcriptome analysis showed that expression of many genes in pearl oyster *Pinctada fucata* significantly increased or decreased during bacterial infection and these genes are involved in multiple immune-related pathways, including chemokine signaling pathway, MAPK signaling pathway, apoptosis, and so on [18]. In razor clam *Sinonovacula constricta*, complement system was identified to be involved in the hepatopancreas defense response to the bacterial challenge [19]. The immune-related differential expression genes were also investigated in *Mytilus coruscus* by transcriptome profiling, and immune-related components were identified, such as TLR-like signaling pathway and MAPK signaling pathway [20]. In addition, the complex immune defense during bacterial infection might affect the metabolism process, which would provide energy for the host defense [21]. Lee et al. found that the metabolic change were induced to response to enteric infection in fruit fly based on RNA-seq, which is necessary for immune defense to enteric infection [22]. During bacterial challenge, immune response and metabolic process must be orchestrated to maintain cellular metabolic homeostasis and provide enough energy for host defense [23–30]. However, the knowledge about the mechanism of immune response and energy metabolism in mollusks is still scarce, which limits our comprehension about the host defense in mollusks after bacterial challenge.

In this study, clams *M. petechialis* were infected by *Vibrio parahaemolyticus* via immersion pattern to simulate a natural infection process. Based on the clam mortality data, samples from four infection phases were applied to comparative transcriptome analysis. Differentially expressed genes and pathways involved in host defense were analyzed to investigate the clam dynamic immune and metabolism changes during bacterial infection. The results will provide the global transcriptome profiles and gain insight into host defense of clams during bacterial infection.

2. Method

2.1. Clams and treatments

Clams (1-year-old) were collected from our cultured population in Wenzhou, China. The clams were acclimated in a 2000 L tank with aerated seawater and fed *Isochrysis galbana* for one week at 28 °C, and then applied to *Vibrio* challenge. A pathogenic *Vibrio parahaemolyticus* strain (MM21) isolated from *M. petechialis* was used in the challenge [4]. The *Vibrio* challenge experiment was performed as described in Liang et al. [31] with slight modification. In detail, clams were randomly divided into two groups, i.e., the control group and challenge group. For the control group, the clams were reared in fresh seawater renewed every day. For the challenge group, the clams were immersed in seawater with 1×10^7 CFU ml^{-1} *V. parahaemolyticus*. The seawater through sand filter and *V. parahaemolyticus* were renewed every day, and the *V. parahaemolyticus* addition was stopped when clam cumulative mortality reached to 10%. The health status of clams was checked every 6 h, and the dead or moribund individuals were picked out at once to avoid fouling the water quality by dead clams. The clam mortalities in the two groups were recorded every day.

The hepatopancreas tissues from 40 clams at each time point in the challenge group were sampled at 0, 1, 2, 3, 5 and 12 days post-infection (dpi), respectively. Each hepatopancreas was divided into two equally parts. One part was frozen in liquid nitrogen for RNA extraction, and the other half was used for *Vibrio* count (data not shown). That is, at each time point, 10 half-hepatopancreas were mixed as one replicate (total of four replicates) for RNA extraction.

2.2. Library construction, sequencing, and quality control

Total RNA was separately extracted from the hepatopancreas mixture of each replicate at each time point post challenge using Trizol (Invitrogen, USA) following the manufacturer's instructions, and was digested with DNase I (Invitrogen, Life Technologies, Carlsbad, CA, USA) to degrade residual genomic DNA. The concentration and quality of RNA was checked by a Nanodrop 2000 spectrophotometer (thermo, USA) and agarose gel electrophoresis (AGE). Besides the hepatopancreas sampled in our challenge experiment (section 2.1), hepatopancreas sampled from other unchallenged clams were also applied to the total RNA extraction. Pooled total RNAs were applied to a library preparation for *de novo* transcriptome sequencing. Thus this *de novo* transcriptome can also be used as the reference transcriptome for our other study. RNA extracted from hepatopancreas of each replicate was applied to library preparation for RNA-seq, respectively.

Library was constructed following manufacturer's recommendation. In brief, mRNA molecules were purified from total RNA using poly-T oligo-attached magnetic beads, and then were fragmented into small pieces using fragmentation reagent. The purified RNA fragments were reverse transcribed to produce double-strand cDNA using random hexamer primers and then ligated to an adapter. The ligation products were amplified by PCR to construct the cDNA sequence library. The cDNA library was subjected to sequencing on the BGISEQ-500 platform (BGI, Shenzhen, China). Clean reads were obtained after filtering reads containing adaptor sequences, more than 5% unknown nucleotides, more than 50% bases with Q-value $\leq$ 20, and low-quality reads.

2.3. De novo transcriptome assembly and gene functional annotation

De novo assembly was performed using Trinity [32] to generate contigs. The TGICL software [33] was used to assemble the unigenes to form a single set of nonredundant unigenes. To acquire comprehensive information on gene functions, assembled unigenes were searched against the Nr (NCBI non-redundant protein sequences), Nt (NCBI nucleotide), KOG (eukaryotic Ortholog Groups), SwissProt (a manually annotated and reviewed protein sequence database), Pfam (Protein family), KEGG (Kyoto Encyclopedia of Genes and Genomes) database using BLASTx and BLASTn with an E-value $< 10^{-5}$. Blast2GO [34] was used for GO (Gene Ontology) annotation with an E-value $< 10^{-5}$ based on the protein annotation results of the Nr database. The transcripts were functionally classified by these databases.

2.4. Sequencing mapping and gene expression quantification

To provide an overview of the expression levels of genes, the assembled *de novo* transcriptome was used as the reference database, and the gene expression level was calculated for each sample. Briefly, clean sequencing reads of each sample were mapped to the reference transcriptome using the Bowtie2 program [35]. The gene expression of each read was quantified using RSEM software [36] with default parameters, and the fragments per kilobase of transcript per million fragments mapped (FPKM) value was used to represent expression abundance of the genes. Then, principal component analysis was performed by R package to show the relationship among the transcriptional expression of all samples.

2.5. Differentially expressed genes (DEGs) analysis

Differential expression analysis between two samples, including 1 dpi vs. 0 dpi, 2 dpi vs. 0 dpi, 3 dpi vs. 0 dpi, 5 dpi vs. 0 dpi, 12 dpi vs. 0 dpi, was performed by DESeq R package software (1.10.1). Adjusted *P* value of 0.001 and log2 (fold_change) of 1 were set as the threshold for significantly differential expression [37]. The KEGG enrichment analysis is useful to map unigenes onto known signaling pathways, while GO enrichment analysis is helpful to describe gene product attributes in all organisms by mapping unigenes to functional categories. Go enrichment analysis and KEGG enrichment analysis of DEGs were performed by the phyper R package to better understand the DEGs function, in which Go terms and signal pathways with false discovery rate

Table 1
Primers used for qRT-PCR in this study.

Siganling pathway	Gene_id	Gene name	Primer sequences 5′ 3′
Toll and Imd signaling pathways	Unigene32846_Mp	*Cactus*	F: TATCCGCAACAGTGAAGG
			R: TTCACAGCCAGATTCAGC
	Unigene41553_Mp	*UBE2D*	F: AAGTGGGTCATCTGGGTT
			R: ACAATGGTCTCCTGCTTT
	Unigene22627_Mp	*GNBP3*	F: TTCCACTGAAACCACCCT
			R: CAACTACGCACGGTACTTTAC
Apoptosis	Unigene5727_Mp	*CTSL*	F: GCAATGGTGGTCTGATGGA
			R: TTGGTTCTTGCTCCGCTTC
	CL2098.Contig1_Mp	*Birc2*	F: TTACTTCGATTGTGGCTTAC
			R: GCTTTGTTTCTTCCCTGTAC
	CL868.Contig1_Mp	*Bcl-xL*	F: ACACTCTGATTGGTGCTCT
			R: TTTATTGACTGCCTTCTCG
Chemokine signaling pathway	Unigene38248_Mp	*NCF1*	F: TACCCAAGAAAGCCAAACC
			R: GTCCGAGTCTTTCTTCCATAA
	Unigene45822_Mp	*ADCY5*	F: GGCGAACATATTACCACTA
			R: AAGTCTAAGGCACTCAACAC
MAPK signaling pathway	CL3532.Contig1_Mp	*Duox*	F: CAAAGAGTGTCTGGTGGTC
			R: ACACCCACTTTCCTTACC
	Unigene6392_Mp	*Rhoj*	F: TAACAGCGGATAAACCAAC
			R: AAACACCGTAGCCACATAA
Other genes	CL2362.Contig3_Mp	*ACP*	F: TTAGCATACGGAGTTGACC
			R: AGTGTCCCAGGGTCCACAA
	Unigene10962_Mp	*Lysozyme*	F: ATCCTAAGCGACCACAATCA
			R: CACAGGCATGTCTCGAATG
	CL8151.Contig2_Mp	*SOD*	F: TTATTACACGCCTGCGACAT
			R: AACCCACAATTCTAACACGAC
	CL8690.Contig2_Mp	*GPx*	F: TTCGCTGATAAACTCGTGG
			R: AACGGATGAGAATCTTTGC
	Unigene41108_Mp	*TLR-4*	F: TTTGGTATGGGAACGCAACT
			R: TCTATCCTCAGCACCTTAA
	CL4237.Contig2_Mp	*C4*	F: TACACCGACAAAGGTAGCG
			R: CCACTGTATTCCAGCCTCA
	CL5748.Contig2_Mp	*ARRDC3*	F: ACTTCCGTAATAATAGCGTGTA
			R: CGTCGTGGAGAAAGAACTAA
	CL7742.Contig2_Mp	*SRK2*	F: AGGGTGTTGAGTGCCTTAG
			R: GTCCTCGTAACTTGTTTCTGG

(FDR) less than 0.01 were considered as the enriched significantly ones. Moreover, The DEGs were clustered by Mfuzz package based on R language to investigate the expression profile of DEGs during the *Vibrio* infection.

2.6. Quantitative real-time PCR (qRT-PCR) analysis

Eighteen randomly selected immune-related DEGs were analyzed by qRT-PCR to verify the expression pattern obtained by RNA-seq. The cDNA (0, 1, 2, 3, 5, 12 dpi) applied to RNA-seq was used as the qRT-PCR template. The primer pairs used to amplify the selected gene was designed using Primer premier 5, and the sequences are listed in Table 1 *β-actin* and *EF1α* were employed as the internal references to normalize the relative expression levels among samples [6]. qRT-PCR was performed in Bio Rad CFX 96 Real time PCR system using SYBR premix (TaKaRa, Japan). Each reaction was performed in triplicate, and the PCR condition were as follows: 95 °C for 30 s and 40 cycles of 95 °C for 5 s, 60 °C for 30 s, followed by the melting curve determination. The relative gene expression was analyzed using the $2^{-\triangle\triangle CT}$ method [38]. All data were expressed as the mean ± standard deviation and applied to *F* text. Then, the data were analyzed by *t*-test using software SPSS version 21.0; when $P < 0.05$, the difference was considered statistically significant.

3. Results

3.1. The clam mortality under V. parahaemolyticus challenge

During the *Vibrio* challenge, the mortality of clams was recorded. As shown in Fig. 1a, no clam died in the control group, while the total mortality rate reached to 80% at 13 dpi in the challenge group. Further analysis of the daily mortality showed that no clam died in 1 and 2 dpi, and the clams began to die from 3 dpi (Fig. 1b). The cumulative mortality of clams reached 10% at 4 dpi, after which the *Vibrio* challenge was stopped. The higher daily mortality occurred at 6 and 7 dpi then decreased thereafter. No clam died after 11 dpi. Based on the characteristic mortality data, the infection and disease process could be divided into four phases: 1) latency phase (1–2 dpi), no dead clam was found; 2) prodrome phase (3–4 dpi), dead clams were sporadically observed; 3) onset phase (5–8 dpi), outbreak death was happened though the pathogen was removed thereafter 4 dpi; 4) recovery phase (9–12 dpi), the clam mortality gradually decreased. Here we chose the key time series (0, 1, 2, 3, 5, 12 dpi) that covered different infection phases for subsequent transcriptome analysis.

3.2. De novo transcriptome assembly and gene annotation

A total of 113.56 M raw reads for reference database was generated based on BGISEQ-500 sequencer and 109.44 M clean reads (SRR9128708) were remained after filtering out low quality reads. For the clean reads, more than 98.52% of the bases had a phred value > 20, and more than 91.95% of them had a phred value > 30. The Trinity software generated 73,129 unigenes with an average length of 968 bp and an N50 of 1697 bp. The standard unigenes were annotated by searching the sequences against the Nr, Pfam, KEGG, Swiss-Prot, KOG, GO and NT databases, which produced 28,184 (38.54%), 22,395 (30.62%), 21,655 (29.61%), 20,610 (28.18%), 18,624 (25.47%), 9744 (13.32%) and 6513 (8.91%) hits respectively (Table 2). There were only 1794 (2.45%) were annotated in all of the databases, and 31,987 (43.74%) were annotated in at least one database. Among the unigenes

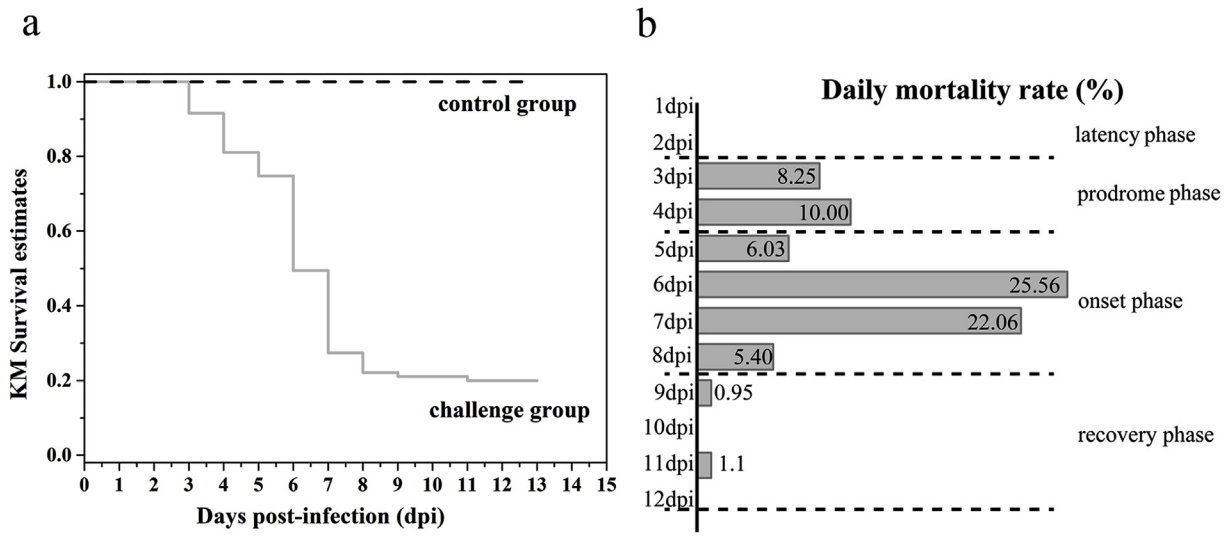

Fig. 1. The diagram of clam mortality in control group and challenge group. **a.** Kaplan-Meier survival estimates for control group and challenge group. The light grey solid line represents for challenge group, and the black dotted line represents for control group. **b.** Daily mortality for challenge group during 12 days of challenge with 1×10^7 CFU ml^{-1} of *V. parahaemolyticus*.

Table 2
The percentage of annotated genes in different database.

Databases	Number of Unigenes	Percentage (%)
Nr	28,184	38.54
Nt	6513	8.91
Swissprot	20,610	28.18
KEGG	21,655	29.61
KOG	18,624	25.47
Pfam	22,395	30.62
Go	9744	13.32
Annotated in all Databases	1794	2.45
Annotated in at least one Databases	31,987	43.74
Total Unigenes	73,129	100

Table 3
Transcriptome summary (number of reads and percentage mapped to the library).

Sample name	Clean read(M)	Total mapping (%)	Uniquely mapping (%)
ck_0d_11G	21.78	83.29	54.95
ck_0d_1G	21.77	82.96	54.76
ck_0d_21G	21.78	83.15	55.65
ck_0d_31G	21.78	83.47	55.17
vp_1d_11G	21.79	83.41	54.05
vp_1d_1G	21.77	83.01	54.37
vp_1d_21G	21.78	83.45	54.45
vp_1d_31G	21.79	84.79	53.94
vp_2d_11G	21.74	84.61	53.66
vp_2d_1G	21.79	84.18	53.49
vp_2d_21G	21.74	84.44	53.04
vp_2d_31G	21.77	84.95	54.28
vp_3d_11G	21.77	83.9	54.52
vp_3d_1G	21.77	83.37	54.22
vp_3d_21G	21.74	84.5	54.3
vp_3d_31G	21.75	84.3	54.68
vp_5d_11G	21.81	84.43	53.55
vp_5d_1G	21.74	84.49	54.23
vp_5d_21G	21.77	83.66	53.84
vp_5d_31G	21.81	83.32	54.63
vp_12d_11G	21.66	83.08	54.05
vp_12d_1G	21.73	82.4	53.92
vp_12d_21G	21.73	82.79	54.2
vp_12d_31G	21.76	82.3	54.55

successfully annotated in the Nr database, the top five species have significantly similarity with *M. petechialis* were *Mizuhopecten yessoensis* (28.51%), *Crassostrea gigas* (17.45%), *C. virginica* (15.47%), *Lottia gigantea* (5.61%) and *Lingula anatin*a (3.58%). Then digital gene expression libraries of the clams collected from four infection phases were sequenced, and sequencing data were deposited in SRA of the NCBI with the accession number [SRR9127709-SRR9127732]. The total clean reads of 24 libraries were mapped respectively to the reference database, and the results were listed in Table 3.

3.3. Overview of the transcriptomic data response to bacterial infection

A principal component analysis (PCA) was performed to obtain a global view on transcriptome profile of clams at different infection phases. The PCA results showed that the first principal component accounts for 76.33% of the variance in the dataset whereas the second one accounts for 15.82% of the variance in the dataset (Fig. 2). A distinct expression profile between the infected clams (1, 2, 3, 5, 12 dpi) and uninfected clams (0 dpi) was observed. It's remarkable that the gene expression of 12 dpi samples (recovery phase) were more similar to that of the 1 dpi samples and 0 dpi. The PCA plot showed that the gene expression information of 2 dpi samples were closer to that of its adjacent time points 1 dpi and 3 dpi samples. Besides, there was some overlap between samples from 3 dpi (blue) and 5 dpi (pink) time points. Moreover, the transcriptome profile of four replicates taken from 5 dpi were more dispersive compared with other time points, whose 95% confidence interval were much bigger than others, indicating that the physiological status of clams from 4 replicates had much differences in the initial onset phase of *Vibrio* infection. The 5 dpi transcriptional profile was consistent with subsequent outbreak death phenotypes that almost one third of these alive samples died at 6 dpi according to the mortality data (Fig. 1b).

The expression level of 70,000 transcripts were compared in clams between each of the infected time points (1 dpi, 2 dpi, 3 dpi, 5 dpi, 12 dpi) and uninfected time point (0 dpi) to find out the DEGs. As a result, a total of 38,067 DEGs were detected. After *Vibrio* infection, a plenty of DEGs were observed at the four infection phases (Fig. 3). Among them, the numbers of DEGs reached to peak value at 2 dpi whereas sharply decreased at 12 dpi after *Vibrio* infection. Taken together, these transcripts response to *Vibrio* infection could be divided into three phases: the acute response phase (1–2 dpi); the maintenance phase (3–5 dpi) and initial recovery phase (12 dpi).

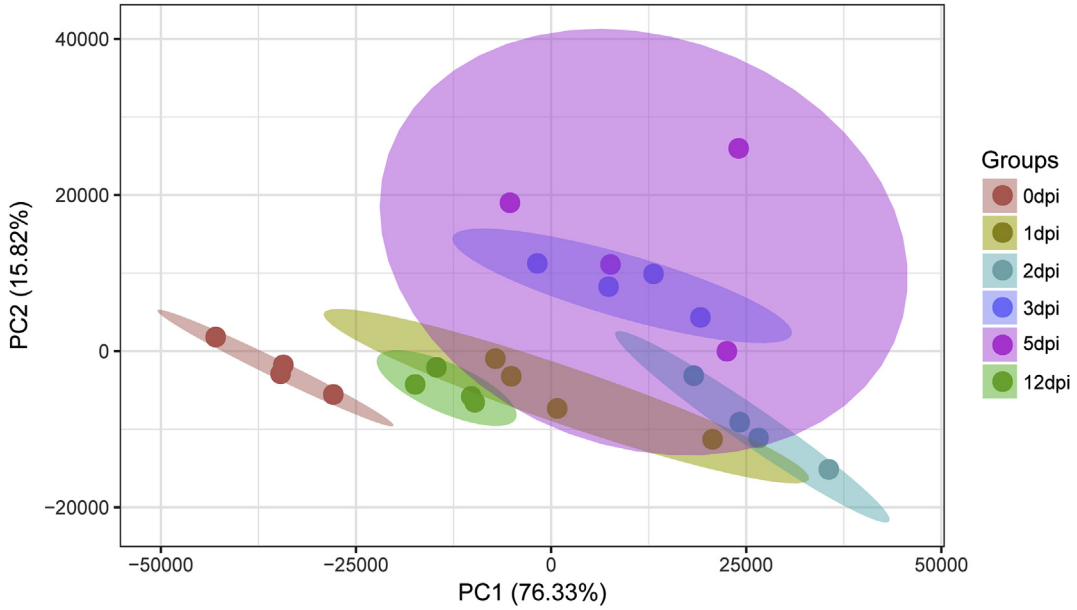

Fig. 2. Principal component analysis (PCA) of golbal gene expression in hepatopancreas response to *V. parahaemolyticus* challenge.

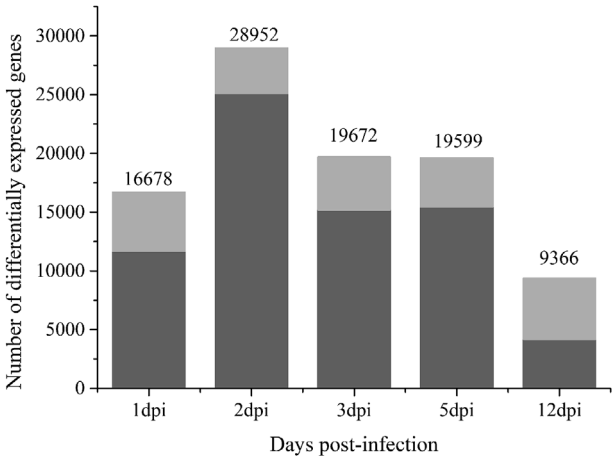

Fig. 3. Number of DEGs in challenge group at 1 dpi, 2 dpi, 3 dpi, 5 dpi, 12 dpi. The DEGs were identified by DEGseq method. The light grey respresents for up-regulated genes, while dark grey respresents for down-regulated genes.

To better understand the function of DEGs, the GO and KEGG analysis were performed to annotate the 38,067 identified DEGs. Go functional enrichment analysis revealed that these DEGs were classified into three GO categories: most significantly “molecular function” (4,058, 10.7%), followed by “cellular component” (3,298, 8.7%), and biological process (2,431, 6.4%). The biological process category contained 15 sub-categories, cellular process (1,571) and metabolic process (1,229) were the top 2 among them (Fig. 4a). In KEGG analysis, the highest numbers of DEGs were related to signal transduction (2,282), cancer overview (1,534), and followed by immune system (1,389) (Fig. 4b). The top 20 KEGG pathways was listed in Supplemental Table S1, and the multiple immune-related signaling pathways, including chemokine signaling pathway (220), NOD-like receptor signaling pathway (298), and RIG-I-like receptor signaling pathway (95) were contained. These findings implied that the hepatopancreas immune system play an important role during bacterial infection. Besides, the pathways associated with metabolism were also significantly enriched, such as carbohydrate metabolism, lipid metabolism, amino acid metabolism, and so on.

3.4. DEGs cluster analysis based on time course

The DEG expression profiles were conducted for cluster analysis to investigate the transcriptional profile response to *V. parahaemolyticus* challenge. The DEGs with little expression (even no expression) at least one time point after bacterial challenge were removed and finally 37,998 DEGs were analyzed with Mfuzz package. The results showed that the expression patterns of all DEGs could be classified into 12 clusters that ranged in size from 1833 to 7014 genes (Fig. 5).

Across the time course, the 12 clusters display three kinds of general pattern: 1) U-shape (38.62%), the genes were subject to transient repression after *Vibrio* challenge, and then normally recuperated to the basal level after 2 dpi or 5 dpi. The clusters displayed different U shapes due to the difference of magnitude and time of genes expression. 2) L-shape (34.62%), the genes were repressed during the whole infection process. Among these clusters, the cluster 5 (7014 DEGs) accounted for the highest proportion in the whole DEGs. 3) inverted-V shape (26.76%), the DEGs in these clusters were all up-regulated against bacterial infection. The genes in clusters 7, 11 and 12 were significantly up-regulated, followed by a return to baseline. Each cluster showed special temporal response to the *Vibrio* infection. For example, the peak expression of cluster 7 and 11 occurred at acute response phase, while the peak expression of cluster 12 occurred at maintenance phase. The genes in cluster 4 showed a rapid and significant up-regulation during bacterial infection. The genes in cluster 6 were not changed at acute and maintenance phase, whereas induced at the initial phase of host recovery from infection.

3.5. Possible roles of DEGs from different expression patterns

The top 20 KEGG signaling pathways enrichment in three kinds of different expression pattern (U-shape, L-shape and inverted V-shape) were listed in Supplemental Table S2. Multiple immune-related signaling pathways were enriched in three kinds of expression pattern, which were involved in killing bacteria, inflammation and apoptosis, etc. Among them, PI3K-Akt signaling pathway, Toll and Imd signaling pathways and TNF signaling pathway were enriched in the inverted V-shape, whereas Natural killer cell mediated cytotoxicity, MAPK signaling pathway and Fc epsilon RI signaling pathway were repressed upon bacterial infection (Fig. 6). The results showed that the immune system would take different strategies including induction expression or

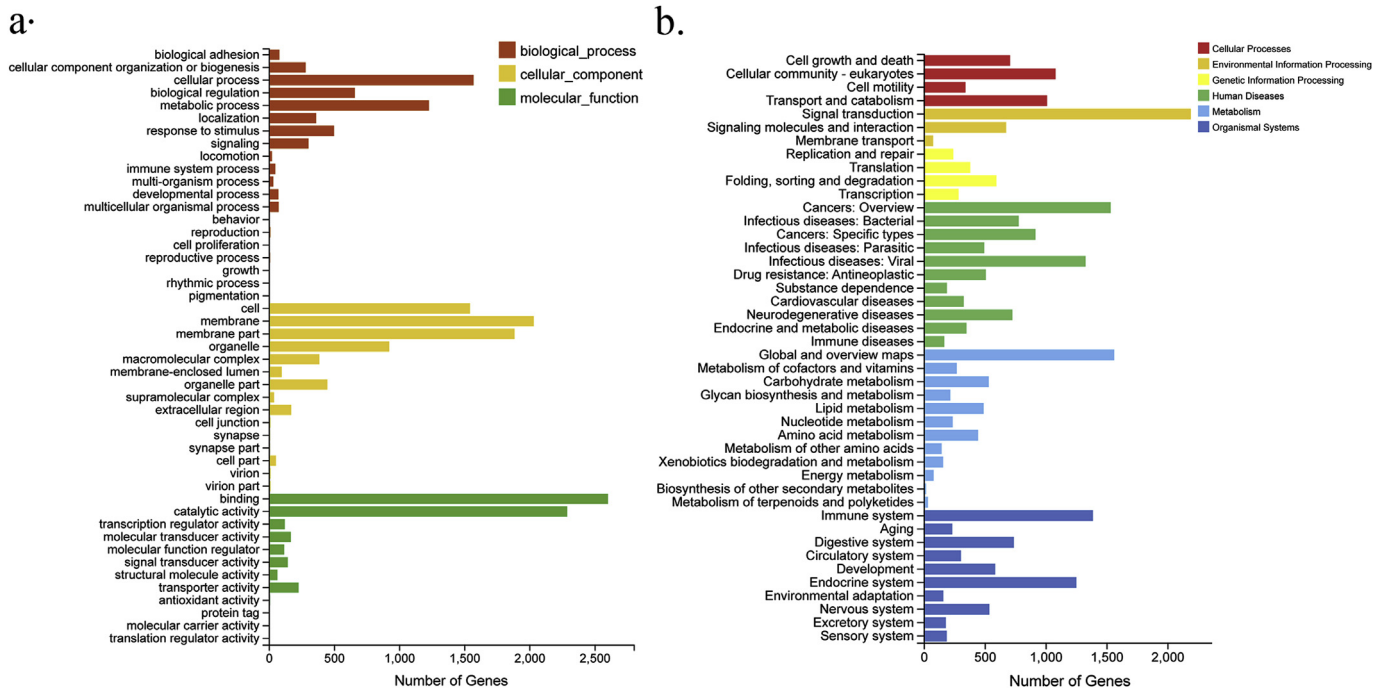

Fig. 4. Infection of *M. petechialis* with *Vibrio* cause the expression of diverse protein. a. Representative protein-based Gene Ontology (Go) for DEGs during *Vibrio* infection. b. KEGG functional classification of DEGs identified from *M. petechialis*.

repression expression to response to bacterial infection.

Several signaling pathways related to anabolism were also enriched in U-shape or L-shape, including mTOR, MAPK, insulin, PI3K-Akt and Wnt signaling pathways (Fig. 6), which were important signaling pathways involved in glycogen, lipid and protein synthesis. While steroid, steroid hormone biosynthesis and PPAR signaling pathway were significantly enriched in the induction expression pattern, which were related to lipid metabolism. Our results showed that multiple signaling pathways related to immune defense and metabolism were affected during *Vibrio* infection, indicating that immunity and metabolic responses might be reprogrammed to protect host, and a trade-off between metabolism and immunity may be a general phenomenon.

3.6. DEGs validation by qPCR

qRT-PCR was conducted to verify the DEGs obtained by RNA-seq. Eighteen DEGs from immune-related signaling pathways, e.g., apoptosis, Toll and Imd signaling pathways, chemokine signaling pathway, MAPK signaling pathway, were selected and applied to qRT-PCR validation. The results showed that the expression profile of most selected genes during the *Vibrio* challenge (16/18) were consistent with that revealed by RNA-seq except for *NCF1*, *ACP,* which confirmed the

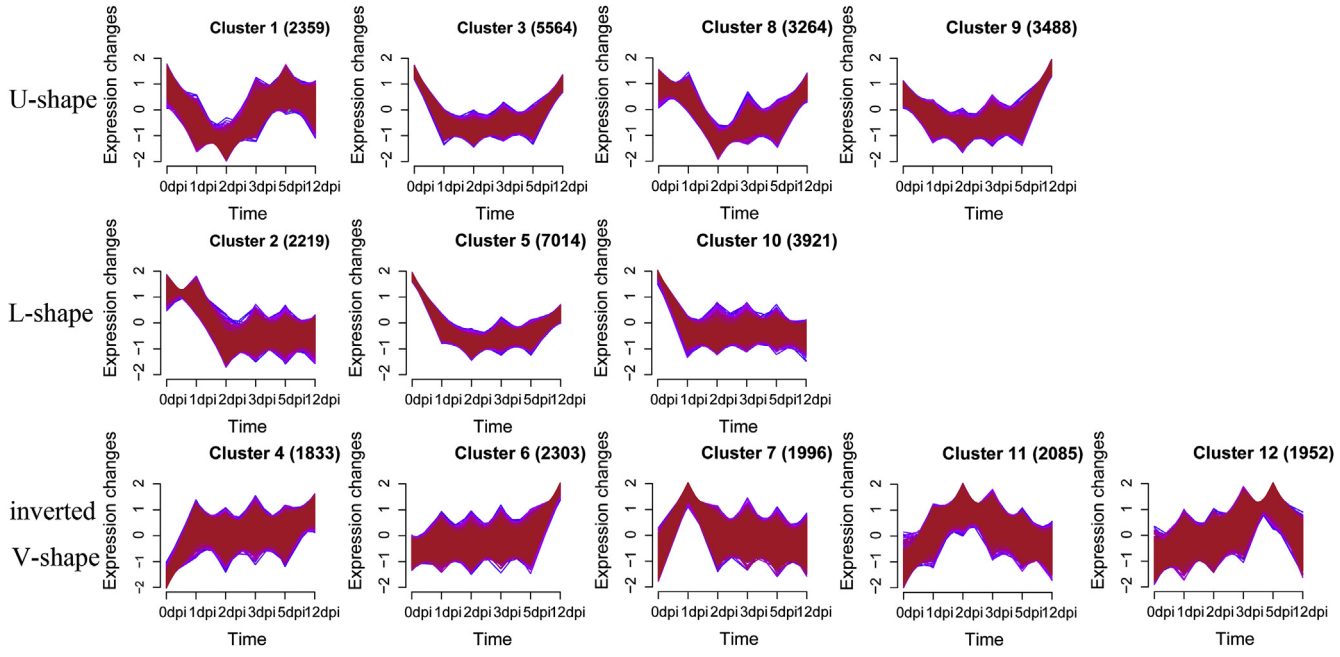

Fig. 5. Clusters of DEGs during different infection time points.

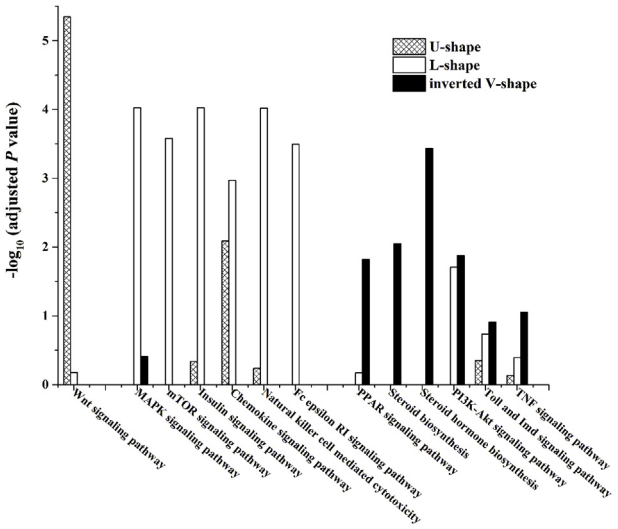

Fig. 6. Immune-related and metabolism-related signaling pathways enriched in top 20 in different expression patterns. The bars represent -$\log_{10}$(Q value) is the significance of the process enriched in three expression patterns.

reliability of RNA-Seq data (Fig. 7).

4. Discussion

A mass mortality caused by *Vibrio* infection has become a major constraint to the clam culture industry. The study focusing on the pathogen and host pathogenesis is the basis for diseases control and genetic breeding of resistance varieties. However, the dynamic response of clams to bacterial infection are largely unknown, although some immune response characters have been reported in *M. petechialis* and other clams after bacterial challenge [6,39]. In the present study, the *M. petechialis* was treated with *Vibrio* via immersion challenge which mimicking the natural infection in seawater. Based on clam mortality data and taking the concept of epidemiology, we divided the disease course after challenge into four phases, including latency, prodrome, onset and recovery phases (Fig. 1). Clam samples from each phase were selected for RNA-seq to analyze the dynamic response of *M. petechialis* hepatopancreas during *V. parahaemolyticus* challenge.

A total 38,067 DEGs were obtained by RNA-seq, in which eighteen DEGs were verified by qRT-PCR, and the expression tendency of the most genes (16/18) were coincident with the RNA-seq. Principal component analysis (PCA) and DEGs up/down-regulation analysis of global gene expression showed that a strong response appeared in clams from 1 dpi to 5 dpi and reduced at 12 dpi. The transcriptome profiles indicating the physiological status of clams fit the daily mortality phenotype at four infection phases. Obviously, the DEG numbers in hepatopancreas sharply increased at latency (1–2 dpi), while kept stable at prodrome and onset phases. The PCA plot showed that the gene expression patterns at adjacent time points were more similar at latency and prodrome phases. At early onset phase, the large differences of the transcriptome profiles among four replicates indicated the different physiological status of the individuals, which might imply different fates of clams (survival or death) in the following time points. Besides, the gene expression of 12 dpi samples were more similar to that of the 0 and 1 dpi samples based on PCA analysis showed the clams at 12 dpi starting to enter the recovery phase. Therefore, the gene expression information is helpful to better understand the physiology status of the clams.

Based on the cluster analysis in Section 3.4, three kinds of expression pattern were significantly clustered, including transient repression then recovery (U-shape), long-lasting repression (L-shape) and induction expression changes (inverted V-shape). According to KEGG functional analysis, immune-related and metabolism-related signaling pathways were enriched separately in three expression patterns. Among them, Toll and Imd signaling pathways, TNF signaling pathway etc. were enriched in induction expression pattern, while chemokine signaling pathway, mTOR signaling pathways, MAPK signaling pathways, Wnt signaling pathways etc. were enriched in repression pattern. The results confirmed that the immune system and metabolism system play important roles in host defense [40], which similar to previous studies [41,42].

Innate immunity is the major way in clams to defense the bacterial infection. Toll and Imd signaling pathways are considered as key pathways involved in the immune response of the invertebrates, which could induce the expression of the antimicrobial peptide (AMP) genes to kill bacteria and fungal [43,44]. In present study, the differential expression of multiple genes in Toll and Imd signaling pathways, such as Cactus, GNBP3 and UBE2D, suggested that Toll and Imd pathways were activated after *Vibrio* infection. Similarly, the Toll and Imd signaling pathways were also reported to play defense roles in the crab *Eriocheir sinensis* against microbial challenge [45]. TNF signaling pathway is critical for mounting innate immunity against bacterial challenge via regulating the cell death or survival [39]. The up-regulation of the genes in TNF signaling pathway in *M. petechialis* after bacterial infection suggested the apoptosis might be promoted to kill the infected cells. PI3K-Akt signaling pathway is related to TLR4-mediated immune defense [46,47], in present study, it was also up-regulated after bacterial infection, similar with the abalone *Haliotis diversicolor* after the *V. parahaemolyticus* stimulation [48]. In contrast, chemokine signaling pathway was enriched significantly in L-shape and the chemokine related genes were down-regulated after infection. Chemokine signaling pathway was reported could traffic and activate leukocytes toward the site of inflammation [49], differential expression of these genes implied that *Vibrio* infection could affect the immune defense by regulating the secretion of chemokines. Taken together, immune related signaling pathways may implement different strategies against bacterial infection.

An anabolism suppression was found in host response to bacterial infection in our study. A plenty of genes involved in the protein synthesis, glycogen synthesis and lipid synthesis were enriched in U-shape or L-shape. The similar results were also found in hard clam *Mercenaria mercenaria,* protein synthesis was inhibited upon parasite infection [50]. In ISE6 tick cells, protein synthesis was also depressed upon *Anaplasma phagocytophilum* infection [51]. In addition, the mTOR and MAPK showed a long-lasting repression expression pattern during bacterial infection. The mTOR signal pathway is an important regulate center for coordination cell growth and metabolism with environmental inputs [52]. The suppression of the mTOR and MAPK pathways implied that the repression of cellular growth and proliferation programs were triggered by bacterial infection. As a result of the inhibition of biosynthesis and gene expression in cellular growth and proliferation, the reduction of ATP demand ensures more energy to be applied to immune defense against bacteria challenge.

At present, a plenty of evidences have shown that the metabolic pathways can directly affect immune cell function, and immune cells also can promote different metabolic pathways in cells [53,54]. In present study, anabolism was transiently or long-term repressed during bacterial infection, and immune defense was also activated in this period. We speculate that the immune cell can autonomously regulate energy influx based on their acute need [30], and then anabolism is changed to provide more energy for host defense. The PI3K-Akt signaling pathway is key regulator of cellular metabolism, and is also involved in immune defense [47,55]. PI3K-Akt signaling pathway was significantly enriched in inverted V-shape in calm *M. petechialis*, suggested immune system and metabolism system were concerted against bacterial infection. The similar result was also found in mouse, in which host defense was affected by glycogen metabolism [56]. The immune and metabolic responses could be orchestrated to maintain homeostasis

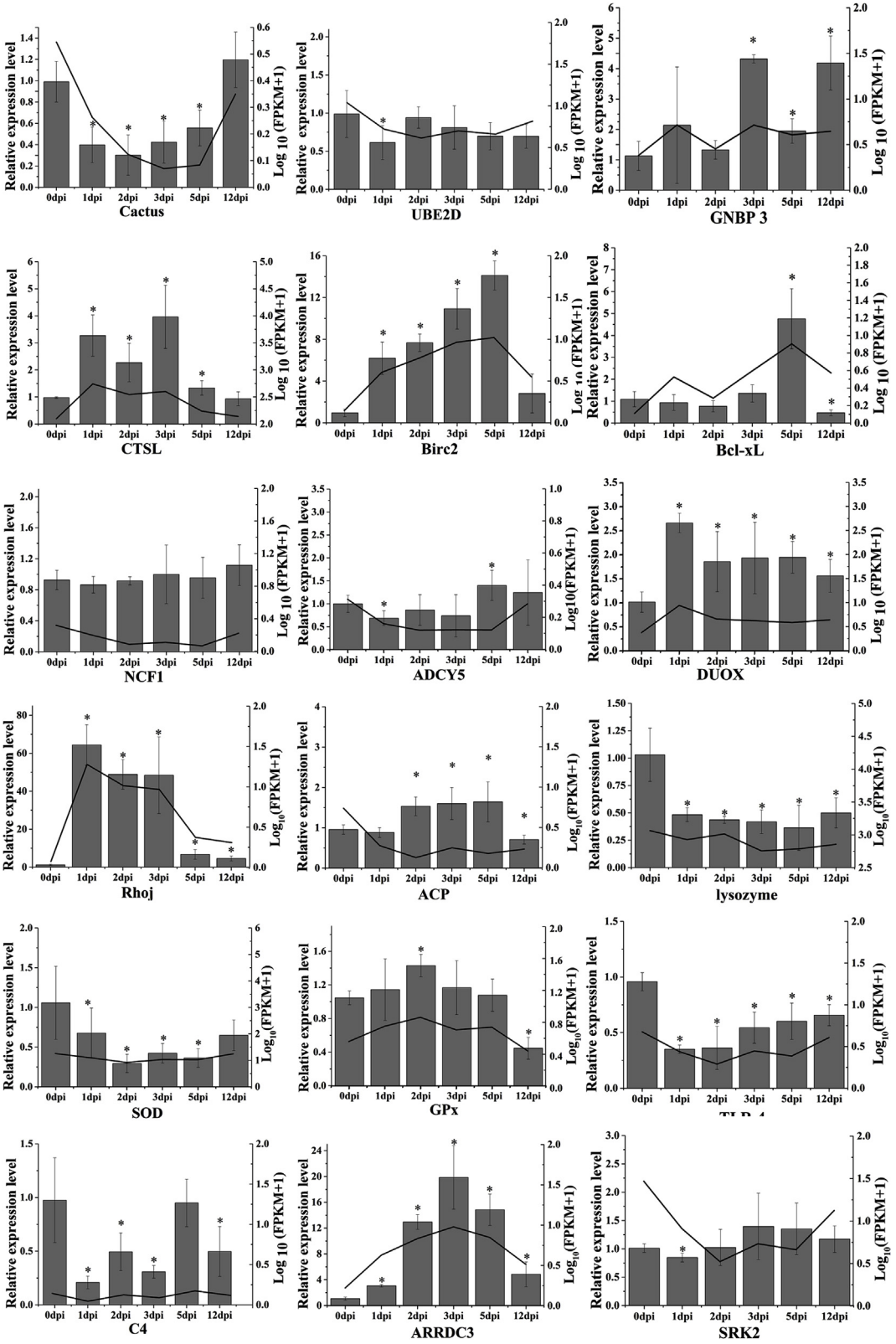

Fig. 7. Expression pattern of selected unigenes by qRT-PCR and RNA-seq. The black line represents the Log_{10}FPKM of selected unigenes at different time points obtained by RNA-seq. The column represents for the fold change of transcript levels at different time points obtained by qRT-PCR. The data obtained by qRT-PCR are expressed as the mean ± SD relative to the reference gene (*β-actin* and *EF1α*). The average expression level at 0 dpi was set to 1. Error bar were calculated based on four biological replicates. * indicates that there is a significant difference in infected samples compared to uninfected samples ($P < 0.05$).

to optimize the performance of immune system and improve host survival.

In conclusion, this study represents the first analysis of the dynamic immune and metabolism response of clam *M. petechialis* during bacterial infection. Although researches on immunometabolism have increased in vertebrate models [57,58], the information is still limited about how interaction of immune and metabolic responses supports host defenses in clam. The results of RNA-seq reveal that immune system and metabolism process are affected by bacterial infection, and they coordinate to participate in the host immune defense. Our study can provide some potential signaling pathways information, and help us to understand the biology underlying these *Vibrio* diseases in molluscan species.

Acknowledgements

This research was supported by the National Natural Science Foundation of China (31772845), the Marine S&T Fund of Shandong Province for Pilot National Laboratory for Marine Science and Technology (Qingdao) (No.2018SDKJ0502-1) and the China Agriculture Research System (CARS-49).

Appendix A. Supplementary data

Supplementary data to this article can be found online at https://doi.org/10.1016/j.fsi.2019.08.057.

References

[1] B. Liu, B. Dong, B. Tang, T. Zhang, J. Xiang, Effect of stocking density on growth, settlement and survival of clam larvae, Meretrix meretrix, Aquaculture 258 (1–4) (2006) 344–349.
[2] B. Tang, B. Liu, G. Wang, T. Zhang, J. Xiang, Effects of various algal diets and starvation on larval growth and survival of *Meretrix meretrix*, Aquaculture 254 (1–4) (2006) 526–533.
[3] B.H. Kim, K.C. Cho, Y.J. Jee, S.G. Byun, M.C. Kim, Growth and survival on enrichment of larvae and early spats of the hard clam, *Meretrix petechialis*, Korean J. Malacol. 27 (4) (2011) 353–358.
[4] X. Yue, B. Liu, J. Xiang, J. Jia, Identification and characterization of the pathogenic effect of a *Vibrio parahaemolyticus*-related bacterium isolated from clam *Meretrix meretrix* with mass mortality, J. Invertebr. Pathol. 103 (2) (2010) 109–115.
[5] X. Yue, B. Liu, L. Sun, Isolation and characterization of a virulent *Vibrio sp.* bacterium from clams (*Meretrix meretrix*) with mass mortality, J. Invertebr. Pathol. 106 (2) (2011) 242–249.
[6] F. Jiang, X. Yue, H. Wang, B. Liu, Transcriptome profiles of the clam *Meretrix petechialis* hepatopancreas in response to *Vibrio* infection, Fish Shellfish Immunol. 62 (2017) 175–183.
[7] K. Buchmann, Evolution of innate immunity: clues from invertebrates via fish to mammals, Front. Immunol. 5 (2014) 459.
[8] U. Muller, P. Vogel, G. Alber, G.A. Schaub, The innate immune system of mammals and insects, Contrib. Microbiol. 15 (2008) 21–44.
[9] J.A.J.M. van de Water, T.D. Ainsworth, W. Leggat, D.G. Bourne, B.L. Willis, M.J.H. van Oppen, The coral immune response facilitates protection against microbes during tissue regeneration, Mol. Ecol. 24 (13) (2015) 3390–3404.
[10] X. Yue, B. Liu, Q. Xue, An i-type lysozyme from the Asiatic hard clam *Meretrix meretrix* potentially functioning in host immunity, Fish Shellfish Immunol. 30 (2) (2011) 550–558.
[11] C. Wang, X. Yue, X. Lu, B. Liu, The role of catalase in the immune response to oxidative stress and pathogen challenge in the clam *Meretrix meretrix*, Fish Shellfish Immunol. 34 (1) (2013) 91–99.
[12] C. Wang, P. Huan, X. Yue, M. Yan, B. Liu, Molecular characterization of a glutathione peroxidase gene and its expression in the selected *Vibrio*-resistant population of the clam *Meretrix meretrix*, Fish Shellfish Immunol. 30 (6) (2011) 1294–1302.
[13] A.T. Tate, A.L. Graham, Dissecting the contributions of time and microbe density to variation in immune gene expression, P Roy. Soc. Lond. B Bio. 284 (1859) 20170727 2017.
[14] Y. Liu, M. Morley, J. Brandimarto, S. Hannenhalli, Y. Hu, E.A. Ashley, W.H. Tang, C.S. Moravec, K.B. Margulies, T.P. Cappola, M. Li, M. consortium, RNA-Seq identifies novel myocardial gene expression signatures of heart failure, Genomics 105 (2) (2015) 83–89.
[15] M. Khalil-Ur-Rehman, L. Sun, C.X. Li, M. Faheem, W. Wang, J.M. Tao, Comparative RNA-seq based transcriptomic analysis of bud dormancy in grape, BMC Plant Biol. 17 (1) (2017) 18.
[16] S. Maekawa, P.C. Wang, S.C. Chen, Comparative study of immune reaction against bacterial infection from transcriptome analysis, Front. Immunol. 10 (2019) 153.
[17] P. Nachappa, J. Levy, C. Tamborindeguy, Transcriptome analyses of *Bactericera cockerelli* adults in response to "*Candidatus* Liberibacter solanacearum" infection, Mol. Genet. Genom. 287 (10) (2012) 803–817.
[18] Z. Wang, B. Wang, G. Chen, J. Jian, Y. Lu, Y. Xu, Z. Wu, Transcriptome analysis of the pearl oyster (*Pinctada fucata*) hemocytes in response to *Vibrio alginolyticus* infection, Gene 575 (2) (2016) 421–428.
[19] X. Zhao, X. Duan, Z. Wang, W. Zhang, Y. Li, C. Jin, J. Xiong, C. Li, Comparative transcriptome analysis of *Sinonovacula constricta* in gills and hepatopancreas in response to *Vibrio parahaemolyticus* infection, Fish Shellfish Immunol. 67 (2017) 523–535.
[20] W. Dong, Y. Chen, W. Lu, B. Wu, P. Qi, Transcriptome analysis of *Mytilus coruscus* hemocytes in response to *Vibrio alginnolyficus* infection, Fish Shellfish Immunol. 70 (2017) 560–567.
[21] T. Roszer, The invertebrate midintestinal gland ("hepatopancreas") is an evolutionary forerunner in the integration of immunity and metabolism, Cell Tissue Res. 358 (3) (2014) 685–695.
[22] K.A. Lee, K.C. Cho, B. Kim, I.H. Jang, K. Nam, Y.E. Kwon, M. Kim, D.Y. Hyeon, D. Hwang, J.H. Seol, W.J. Lee, Inflammation-modulated metabolic reprogramming is required for DUOX-dependent gut immunity in *Drosophila*, Cell Host Microbe 23 (3) (2018) 338–352 e5.
[23] A. Galenza, E. Foley, Immunometabolism: insights from the *Drosophila* model, Dev. Comp. Immunol. 94 (2019) 22–34.
[24] N. Zmora, S. Bashiardes, M. Levy, E. Elinav, The role of the immune system in metabolic health and disease, Cell Metabol. 25 (3) (2017) 506–521.
[25] X. Wang, L. Wang, C. Yao, L. Qiu, H. Zhang, Z. Zhi, L. Song, Alternation of immune parameters and cellular energy allocation of *Chlamys farreri* under ammonia-N exposure and *Vibrio anguillarum* challenge, Fish Shellfish Immunol. 32 (5) (2012) 741–749.
[26] X. Wang, L. Wang, H. Zhang, Q. Ji, L. Song, L. Qiu, Z. Zhou, M. Wang, L. Wang, Immune response and energy metabolism of *Chlamys farreri* under *Vibrio anguillarum* challenge and high temperature exposure, Fish Shellfish Immunol. 33 (4) (2012) 1016–1026.
[27] S. Plana, G. Sinquin, P. Maes, C. Paillard, M. Le Pennec, Variations in biochemical composition of juvenile *Ruditapes philippinarum* infected by a *Vibrio sp*, Dis. Aqua.Organ. 24 (3) (1996) 205–213.
[28] B.A. Seibel, N.S. Hafker, K. Trubenbach, J. Zhang, S.N. Tessier, H.O. Portner, R. Rosa, K.B. Storey, Metabolic suppression during protracted exposure to hypoxia in the jumbo squid, *Dosidicus gigas*, living in an oxygen minimum zone, J. Exp. Biol. 217 (14) (2014) 2555–2568.
[29] M. Erk, D. Ivankovic, Z. Strizak, Cellular energy allocation in mussels (*Mytilus galloprovincialis*) from the stratified estuary as a physiological biomarker, Mar. Pollut. Bull. 62 (5) (2011) 1124–1129.
[30] A. Bajgar, K. Kucerova, L. Jonatova, A. Tomcala, I. Schneedorferova, J. Okrouhlik, T. Dolezal, Extracellular adenosine mediates a systemic metabolic switch during immune response, PLoS Biol. 13 (4) (2015) e1002135.
[31] B. Liang, F. Jiang, S. Zhang, X. Yue, H. Wang, B. Liu, Genetic variation in vibrio resistance in the clam *Meretrix petechialis* under the challenge of *Vibrio parahaemolyticus*, Aquaculture 468 (2017) 458–463.
[32] M.G. Grabherr, B.J. Haas, M. Yassour, J.Z. Levin, D.A. Thompson, I. Amit, X. Adiconis, L. Fan, R. Raychowdhury, Q. Zeng, Full-length transcriptome assembly from RNA-Seq data without a reference genome, Nat. Biotechnol. 29 (7) (2011) 644.
[33] G. Pertea, X. Huang, F. Liang, V. Antonescu, R. Sultana, S. Karamycheva, Y. Lee, J. White, F. Cheung, B. Parvizi, J. Tsai, J. Quackenbush, TIGR gene indices clustering tools (TGICL): a software system for fast clustering of large EST datasets, Bioinformatics 19 (5) (2003) 651–652.
[34] A. Conesa, S. Gotz, J.M. Garcia-Gomez, J. Terol, M. Talon, M. Robles, Blast2GO: a universal tool for annotation, visualization and analysis in functional genomics research, Bioinformatics 21 (18) (2005) 3674–3676.
[35] B. Langmead, S.L. Salzberg, Fast gapped-read alignment with Bowtie 2, Nat. Methods 9 (4) (2012) 357–359.
[36] B. Li, C.N. Dewey, RSEM: accurate transcript quantification from RNA-Seq data with or without a reference genome, BMC Bioinf. 12 (1) (2011) 323.
[37] L. Wang, Z. Feng, X. Wang, X. Wang, X. Zhang, DEGseq: an R package for identifying differentially expressed genes from RNA-seq data, Bioinformatics 26 (1) (2010) 136–138.
[38] K.J. Livak, T.D. Schmittgen, Analysis of relative gene expression data using real-time quantitative PCR and the 2(-Delta Delta C(T)) Method, Methods 25 (4) (2001) 402–408.
[39] Y. Ren, J. Xue, H. Yang, B. Pan, W. Bu, Transcriptome analysis of *Ruditapes philippinarum* hepatopancreas provides insights into immune signaling pathways under *Vibrio anguillarum* infection, Fish Shellfish Immunol. 64 (2017) 14–23.
[40] B.H. Nam, M. Jung, S. Subramaniyam, S.I. Yoo, K. Markkandan, J.Y. Moon, Y.O. Kim, D.G. Kim, C.M. An, Y. Shin, H.J. Jung, J.H. Park, Transcriptome analysis revealed changes of multiple genes involved in *Haliotis discus* hannai innate immunity during *Vibrio parahemolyticus* infection, PLoS One 11 (4) (2016) e0153474.
[41] Y. Mu, F. Ding, P. Cui, J. Ao, S. Hu, X. Chen, Transcriptome and expression profiling analysis revealed changes of multiple signaling pathways involved in immunity in the large yellow croaker during *Aeromonas hydrophila* infection, BMC Genomics 11 (1) (2010) 506.
[42] C.Y. Chin, D.M. Monack, S. Nathan, Genome wide transcriptome profiling of a murine acute melioidosis model reveals new insights into how *Burkholderia pseudomallei* overcomes host innate immunity, BMC Genomics 11 (1) (2010) 672.
[43] F. Li, J. Xiang, Signaling pathways regulating innate immune responses in shrimp, Fish Shellfish Immunol. 34 (4) (2013) 973–980.
[44] H. Myllymaki, S. Valanne, M. Ramet, The *Drosophila* imd signaling pathway, J. Immunol. 192 (8) (2014) 3455–3462.

[45] X. Li, Z. Cui, Y. Liu, C. Song, G. Shi, Transcriptome analysis and discovery of genes involved in immune pathways from hepatopancreas of microbial challenged mitten crab *Eriocheir sinensis*, PLoS One 8 (7) (2013) e68233.
[46] T. Fukao, S. Koyasu, PI3K and negative regulation of TLR signaling, Trends Immunol. 24 (7) (2003) 358–363.
[47] B. Mattioli, L. Giordani, M.G. Quaranta, M. Viora, Leptin exerts an anti-apoptotic effect on human dendritic cells via the PI3K-Akt signaling pathway, FEBS Lett. 583 (7) (2009) 1102–1106.
[48] Y. Sun, X. Zhang, G. Wang, S. Lin, X. Zeng, Y. Wang, Z. Zhang, PI3K-AKT signaling pathway is involved in hypoxia/thermal-induced immunosuppression of small abalone *Haliotis diversicolor*, Fish Shellfish Immunol. 59 (2016) 492–508.
[49] J.E. Pease, T.J. Williams, The attraction of chemokines as a target for specific anti-inflammatory therapy, Br. J. Pharmacol. 147 (Suppl 1) (2006) S212–S221.
[50] K. Wang, E. Pales Espinosa, A. Tanguy, B. Allam, Alterations of the immune transcriptome in resistant and susceptible hard clams (*Mercenaria mercenaria*) in response to Quahog Parasite Unknown (QPX) and temperature, Fish Shellfish Immunol. 49 (2016) 163–176.
[51] M. Villar, N. Ayllon, P. Alberdi, A. Moreno, M. Moreno, R. Tobes, L. Mateos-Hernández, S. Weisheit, L. Bell-Sakyi, J. de la Fuente, Integrated metabolomics, transcriptomics and proteomics identifies metabolic pathways affected by *Anaplasma phagocytophilum* infection in tick cells, Mol. Cell. Proteom. 14 (12) (2015) 3154–3172.
[52] M. Laplante, D.M. Sabatini, mTOR signaling in growth control and disease, Cell 149 (2) (2012) 274–293.
[53] L.A. O'Neill, R.J. Kishton, J. Rathmell, A guide to immunometabolism for immunologists, Nat. Rev. Immunol. 16 (9) (2016) 553–565.
[54] R.M. Loftus, D.K. Finlay, Immunometabolism: cellular metabolism turns immune regulator, J. Biol. Chem. 291 (1) (2016) 1–10.
[55] Y. Liu, R. Wang, L. Zhang, J. Li, K. Lou, B. Shi, The lipid metabolism gene FTO influences breast cancer cell energy metabolism via the PI3K/AKT signaling pathway, Oncol. Lett. 13 (6) (2017) 4685–4690.
[56] P.M. Thwe, L. Pelgrom, R. Cooper, S. Beauchamp, J.A. Reisz, A. D'Alessandro, B. Everts, E. Amiel, Cell-intrinsic glycogen metabolism supports early glycolytic reprogramming required for dendritic cell Immune responses, Cell Metabol. 26 (3) (2017) 558–567 e5.
[57] A. Wang, H.H. Luan, R. Medzhitov, An evolutionary perspective on immunometabolism, Science 363 (6423) (2019) eaar3932.
[58] Y.S. Lee, J. Wollam, J.M. Olefsky, An integrated view of immunometabolism, Cell 172 (1–2) (2018) 22–40.